Received: 23 March 2023 | Revised: 12 January 2024 | Accepted: 20 February 2024

DOI: 10.1002/ecy.4304

ARTICLE

ECOLOGY
ECOLOGICAL SOCIETY OF AMERICA

# Spawning fish maintains trophic synchrony across time and space beyond thermal drivers

**Anders Frugård Opdal**[1] | **Peter J. Wright**[2] | **Geir Blom**[3] | **Hannes Höffle**[4] | **Christian Lindemann**[1,5] | **Olav Sigurd Kjesbu**[6]

[1]Department of Biological Sciences, University of Bergen, Bergen, Norway

[2]Marine Scotland Science, Aberdeen, UK

[3]Department of Statistics, Directorate of Fisheries, Bergen, Norway

[4]Institute of Marine Research, Tromsø, Norway

[5]Marine Biology Section, The Norwegian Institute for Water Research, Bergen, Norway

[6]Institute of Marine Research, Bergen, Norway

**Correspondence**
Anders Frugård Opdal
Email: anders.opdal@uib.no

**Funding information**
H2020 Society, Grant/Award Number: 817806; Norges Forskningsråd, Grant/Award Numbers: 15078, 287490

**Handling Editor:** Lorenzo Ciannelli

## Abstract

Increasing ocean temperature will speed up physiological rates of ectotherms. In fish, this is suggested to cause earlier spawning due to faster oocyte growth rates. Over time, this could cause spawning time to become decoupled from the timing of offspring food resources, a phenomenon referred to as trophic asynchrony. We used biological data, including body length, age, and gonad developmental stages collected from >125,000 individual Northeast Arctic cod (*Gadus morhua*) sampled between 59 and 73° N in 1980–2019. Combined with experimental data on oocyte growth rates, our analyses show that cod spawned progressively earlier by about a week per decade, partly due to ocean warming. It also appears that spawning time varied by more than 40 days, depending on year and spawning location. The significant plasticity in spawning time seems to be fine-tuned to the local phytoplankton spring bloom phenology. This ability to partly overcome thermal drivers and thus modulate spawning time could allow individuals to maximize fitness by closely tracking local environmental conditions important for offspring survival. Our finding highlights a new dimension for trophic match–mismatch and should be an important consideration in models used to predict phenology dynamics in a warmer climate.

**KEYWORDS**
climate change, phenology, physiology, phytoplankton, temperature, trophic synchrony

## INTRODUCTION

With climate warming, events in spring, such as flowering, insect bursts, egg laying, spawning, and migrations, are found to occur earlier (Parmesan, 2007; Poloczanska et al., 2013). When ambient temperatures increase, metabolic and developmental rates in both plants and ectothermic organisms speed up, advancing phenological events. Differences in the rate of change are suggested to cause trophic asynchrony (Asch et al., 2019; Both et al., 2009; Durant et al., 2007; Thackeray et al., 2016; Winder & Schindler, 2004), such as that between bird hatch date and insect food availability (Both et al., 2006) or between zooplankton abundance and its phytoplankton prey (Edwards & Richardson, 2004).

Generally, trophic synchrony is a key life-history principle in high-latitude ecosystems due to seasonal differences and a pulsed planktonic production in spring

(Cushing, 1990; Hjort, 1914; Hughes, 2000), referred to as spring bloom systems (Sundby et al., 2016). During winter, nutrient concentrations are high, but phytoplankton growth is constrained by short days and a deep mixed layer, constantly moving phytoplankton out of the shallow euphotic zone. As spring approaches, with days becoming longer, temperature rising, and the water column stabilizing, phytoplankton is retained in the euphotic zone, and the spring bloom starts (Doney, 2006; Lindemann & St. John, 2014; Sverdrup, 1953). In turn, this event triggers zooplankton spawning, like that for the abundant calanoid copepod *Calanus finmarchicus* (Melle et al., 2014) whose eggs and nauplii are important prey for the newly hatched fish larvae (Beaugrand et al., 2003; Cushing, 1990; Opdal & Vikebø, 2016). This sequence of events is also supported by field studies linking good or poor recruitment success in fish with a match or mismatch between phytoplankton bloom timing and fish spawning time, respectively (Malick et al., 2015; Platt et al., 2003; Schweigert et al., 2013).

One explanation for the apparent increase in the occurrence of trophic asynchrony (mismatch) in spring bloom systems (Poloczanska et al., 2013) is that temperature has a direct physiological effect on fish spawning phenology (Kjesbu et al., 2010; Neuheimer & MacKenzie, 2014; Pankhurst & Munday, 2011) but affects phytoplankton phenology only indirectly, mainly through environmental drivers like stratification (Asch et al., 2019; Doney, 2006). Thus, with climate warming, we should, at least in principle, expect a gradual decoupling between the timing of fish spawning and the timing of the phytoplankton spring bloom (Asch et al., 2019; Poloczanska et al., 2013). However, when it comes to marine systems, evidence for this is limited (Edwards & Richardson, 2004), likely due to the lack of high-quality phenological time series (Atkinson et al., 2015; Samplonius et al., 2021).

Atlantic cod, *Gadus morhua*, has been a key species in the development of the match–mismatch hypothesis, as they spawn around the time of the spring bloom and the stocks have undergone significant changes in recruitment linked to climate change (Beaugrand et al., 2003; Kjesbu et al., 2023; Kristiansen et al., 2011). Originally, the match–mismatch hypothesis implicitly assumes a near-constant fish spawning time across years and where variable timing of food availability for the fish larvae is driven by interannual fluctuations in phytoplankton bloom timing (Cushing, 1969, 1990). However, Pedersen (1984) found a significant 2-week delay in Northeast Arctic (NEA) cod spawning time, apparently unrelated to temperature. Also, when comparing cod populations, it has been suggested that cues other than temperature can come into play to tune spawning behavior to match local environmental conditions (Neuheimer et al., 2018; Neuheimer & MacKenzie, 2014).

In this study, we seek to further untangle the relative importance of individual plasticity from generally defined, temperature-driven physiological rates on determining the time of spawning, using the data-rich NEA cod as a case in point. The NEA cod have their feeding and nursery areas in the Barents Sea, and when they reach sexual maturity, they start undertaking more or less annual spawning migrations (up to 2400 km) to spawning grounds along the Norwegian coast (Opdal & Jørgensen, 2015). Depending on distance to spawning ground, migration typically starts in late autumn/early winter, and spawning takes place between late winter/early spring the following year (Bergstad et al., 1987).

The present biological data set includes age, length, sex, and gonad developmental stage of 126,491 individual NEA cod caught along the Norwegian coast (59.3–72.8° N) between 1980 and 2019. After this data collation, we applied a mechanistic model to back-calculate the temperature histories for cod spawning at different locations. Together with spatially resolved phytoplankton concentrations (1998–2019), we could then isolate the effect of temperature-driven oocyte growth (vitellogenic) rates on spawning time from other effects, such as that of the timing of the local phytoplankton spring bloom. Lastly, we combined this extensive field information with a reanalysis of experimental reproductive data sets (Kjesbu et al., 2010) focusing on individual instead of average oocyte growth rates to investigate the potential for plasticity in spawning time.

## MATERIALS AND METHODS

### Individual data

Data on individual cod were collected by the Institute of Marine Research (IMR) between 1980 and 2019 from three standardized sampling schemes: regular scientific surveys, commercial port samples, and the coastal reference fleet. The latter consists of around 20 vessels in the Norwegian coastal fishing fleet (9–15 m length), contracted by the IMR since 2005 to collect biological information from catches, and is representative of the coastal fishing fleet as a whole (Fangel et al., 2015; Moan et al., 2020). The commercial port sampling has taken place year-round at landing sites along the Norwegian coast north of 62° N since 1980 using a chartered vessel, operated by the IMR. All three sampling programs collect the same type of biological information and have adopted the same methodological standards throughout the period. Here, we utilized data on NEA cod collected

through all programs and within 350 km of the Norwegian coastline.

The combined data set (Opdal et al., 2023) contains a total of 6657 unique sampling events, with a mean of 19 randomly sampled NEA cod per station, totaling 126,491 individuals across all years (Figure 1). For each sampled individual, the total length (Length) was measured to the nearest centimeter below, and gonad development (maturity) stage (Stage) was classified macroscopically in five stages: immature, maturing, spawning, spent/resting, and uncertain. In this study, we only considered maturing and spawning stages and denote them by Stage = 0 and Stage = 1, respectively. Further, the otolith growth increments were counted to provide the age (Age) (Denechaud et al., 2021; Rollefsen, 1933). In addition to biological data, the data set also includes information on year (Year), day of year (Doy), gear type (Gear), and geographic coordinates

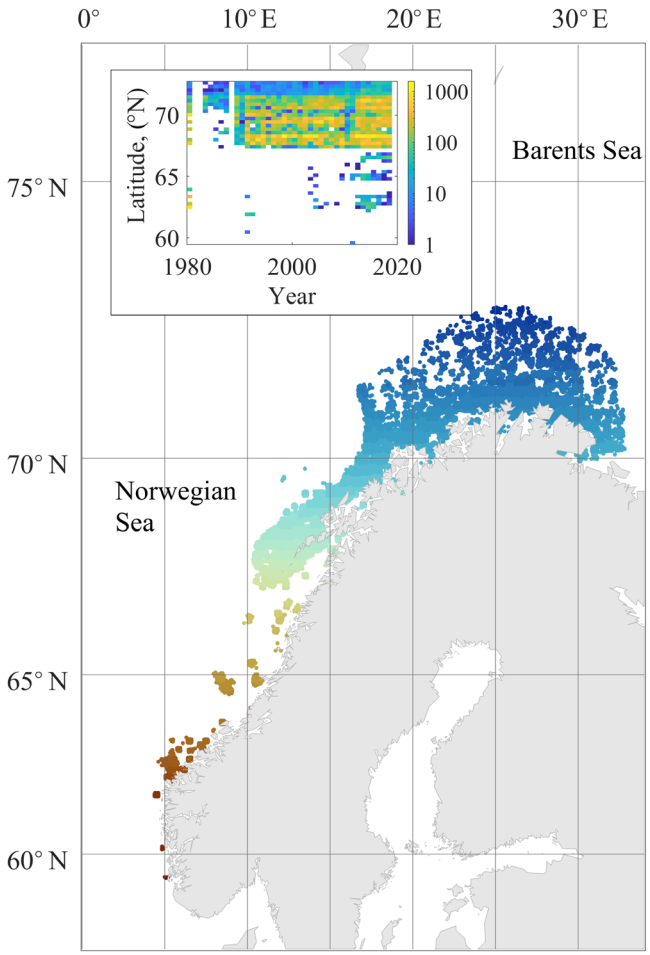


**FIGURE 1** Catch locations for the 126,491 individual Northeast Arctic cod sampled between 1980 and 2019. Dots indicate location, color denotes latitude of corresponding 25 × 25-km grid cell to which they are assigned. Inserted bar plot shows number of fish sampled at each year and grid latitude.

for each sampling location (Lat and Lon) (Figure 1). The latter was also transposed to UTM coordinates ($X$, $Y$) to achieve an isotropic form needed for the statistical analyses. The years 1981, 1982, and 1988 were missing information on one or more of the aforementioned variables and could not be included in further analyses.

## Statistical prediction of spawning time

To identify interannual and spatial differences in spawning time, we constructed a logistic binomial generalized additive model using the statistical software program R version 4.3.1 with the mgcv library 1.8-38 (Wood et al., 2016). The model was based on the day of year (Doy) of the maturing (Stage = 0) and spawning (Stage = 1) stages—prescribing Stage as a logistic function of Doy. In addition, auxiliary explanatory variables were included as either a spline-based smooth ($s$; $X$, $Y$, basis function [bs] = thin plate [tp]), a tensor product smooth ($te$; Length, Age, basis function [bs] = cubic regression [cr]), or factorial variables ($F$; Year and Gear), such that

$$\begin{aligned}\text{Stage} = \text{Doy} + s(X,Y) + te(\text{Age},\text{Length}) + F_1(\text{Year}) \\ + F_2(\text{Gear}),\end{aligned} \quad (1)$$

with family = binomial, link function = logit. Although Gear is not expected to influence maturity stage, it was included to account for any temporal and regional variation in gear use. For both the tensor product smooth ($te$(Age, Length), initial basis size $k' = 25$) and the spline-based smooth ($s$($X$, $Y$), initial basis size $k' = 150$), a penalized likelihood was applied to estimate the respective basis dimensions ($k$). However, for the latter, estimated $k$ was similar to the initial basis size ($k'$), and thus we investigated a series of different initial basis sizes ($k' = 10,\ 20,\ 50,\ 150$) to check the sensitivity to this constraint. Finally, a model selection procedure was performed comparing models with all combinations of predictor variables using the Akaike information criterion (AIC). The model with the lowest AIC was selected.

The selected model was then used to make a statistical prediction of the day of year on which there was a 50% probability of gonad stage being in spawning state (Stage = 1) at a given location ($X$, $Y$) and year (Year) and for a fixed set of auxiliary predictor values (Age, Length, and Gear). Model predictions were made for all sampled years (1980–2019), but not for all sampled locations ($X$, $Y$). Since spawning individuals (Stage = 1) were sampled at >2500 unique locations, we constrained predictions to a 25 × 25-km grid, giving a total of 253 locations. Predictions at finer (10 × 10-km) and

coarser (50 × 50-km and 200 × 200-km) grids were also done to investigate potential sensitivity to grid resolution.

## Relative spawning time derived from oocyte development rates

The timing of spawning is tightly connected to the oocyte development time, which again is driven by the ambient-temperature history during vitellogenesis ($T_{VIT}$) (Kjesbu et al., 2010). Thus, with information on the daily ($t$) $T_{VIT}$ history prior to spawning (see next paragraph) and a corresponding estimate of daily oocyte development rate ($R(t)$, in micrometers per day), we can calculate the theoretical temperature-driven oocyte development time (number of days from start of vitellogenesis to spawning). This development time will be longer in cold temperatures and shorter in warm temperatures and is a relative measure of temperature-predicted spawning time, assuming that spawning time is dependent on oocyte development time (Asch et al., 2019; Kjesbu et al., 2010; Pankhurst & Munday, 2011). This means that for each statistical prediction of spawning time (Equation 1, for each grid cell and year), we can estimate the corresponding temperature-predicted oocyte development time. While this approach does not predict the date of spawning (since the start date of oocyte development is unknown), it does provide a relative measure of the variation in spawning time between grid cells and between years. This, in turn, allows us to compare the statistical predictions of spawning time (Equation 1) to the corresponding mechanistic temperature-predicted relative spawning times (Equation 2, below).

We used the daily ($t$) temperature-driven oocyte growth rates ($R(t)$, in micrometers per day) as described in the experimental study of Kjesbu et al. (2010) on coastal cod. In short, to find $R(t)$, individual oocyte growth trajectories were established by repeated ovarian biopsies (on the same fish) held at two different temperatures (5 and 9.3°C) over the course of 4 months (October–January). For each biopsy, the oocyte diameter of the 5% largest oocytes (leading cohort) was measured. The resulting $R(t)$ is thus the daily ($t$) average oocyte growth (in micrometers) at temperature ($T_{VIT}$, in degrees Celsius):

$$R(t) = 4.21 \times 1.44^{\frac{T_{VIT}(t) - 9.6}{10}}, \quad (2)$$

where 4.21 refers to the average $R$ between the two temperature experiments and 1.44 to the $Q_{10}$-value. Note that this equation fails above 9.6°C, that is, when reproductive problems (like lower egg fertilization rates) start to occur in this species in too warm waters (van der Meeren & Ivannikov, 2006). Thus, the threshold 9.6°C refers to the upper pejus temperature for ovulation (Kjesbu et al., 2023).

Using Equation (2), we back-calculated the time it takes for the first group of oocytes (leading cohort, LC) to grow backwards from 690 μm, which is considered to be shortly before oocyte hydration (swelling) and first spawning, to a minimum diameter of 250 μm, reflecting the initiation of the reproductive cycle (vitellogenesis) (Kjesbu et al., 2010). This back-calculation begins at the statistically predicted spawning time (Equation 1, for each grid cell and year) and runs backwards in time and space, updating $T_{VIT}$ each day.

To obtain a field-based estimate for $T_{VIT}$, we first calculated the shortest swimming route from the Barents Sea to each possible spawning location (grid cell) and used this route, together with assumed swimming speeds (see below), to extract daily temperatures from a numerical ocean model. The spawning migration routes between the center of gravity of the NEA cod in the central Barents Sea (75° N, 35° E; Kjesbu et al., 2023), and each grid cell along the Norwegian coastline was calculated using the A* search algorithm (Hart et al., 1968) implemented by the "plannerAStarGrid" function in MATLAB 2023 and applied to a 4 × 4-km map grid. This exercise resulted in a total of 253 unique spawning migration routes, one from each of the 25 × 25-km grid cells and assumes that all fish select the shortest route from the common starting point in the Barents Sea.

Daily temperature fields were drawn from a numerical ocean hindcast archive for the Nordic Seas (Lien et al., 2013, 2014). The archive was established with a regional ocean model system (ROMS) on a 4 × 4-km-resolution grid with 32 sigma layers. The model is known to compare well with repeated measurements of temperature and salinities along the Norwegian coast (Lien et al., 2013, 2014). By combining the migration route and temperature fields, a daily $T_{VIT}(t)$ trajectory was retrieved by backward calculation, starting at the statistical model prediction of spawning day (Equation 1) in each year and grid cell and moving backward (northward) along the migration route to the central Barents Sea. Because vertical movement is not modeled, temperature fields were averaged at depths between 50 and 350 m, which is the typical depth range of NEA cod as observed from data storage tags (DSTs) (Godø & Michalsen, 2000). Once in the Barents Sea, daily temperatures were updated by randomly drawing from the temperature distribution (mean ± 2 SDs) within a 130-km radius.

To determine reasonable swimming speeds ($v$), we started by using information of observed $T_{VIT}$ derived from six DSTs recaptured along the Finnmark coast (69.9–71.7° N) in 1997 (Godø & Michalsen, 2000). For all

modeled migration routes ending between these two latitudes (migration distance, $d = 450$–$850$ km), we estimated the swimming speed $v_{DST}$ (in kilometers per day) that yielded a back-calculated $T_{VIT}$ in 1996–1997 as close as possible to that observed from the DSTs. The initial swimming speed assumption (V1) was then set so that $v(d) = v_{DST}$. In addition, we tested four alternative assumptions (V2–V5) where the speed was dependent on migration distance ($d$), such that $v(d) = \beta + \alpha \times d$. Here, parameter selection was constrained to ensure that average $v(d = 450$–$850\text{ km}) \approx v_{DST}$.

## Phytoplankton spring bloom onset

The spring bloom onset was derived from satellite images of surface chlorophyll *a* (chl *a*) concentration estimates (in megagrams per cubic meter) available through the Copernicus Marine Service (European Union). Specifically, we opted for the chl *a* concentration product (CHL) from the Global Ocean Color level-3 multisensor product with daily gap-free estimates at a spatial grid resolution of 4 × 4 km, available from the first full year in 1998 (https://doi.org/10.48670/moi-00280). This product is known to perform well in comparison with in situ measurements (Garnesson & Bretagnon, 2022). For each 25 × 25-km grid cell, daily chl *a* concentration was calculated as the average across the corresponding thirty 4 × 4-km CHL grid cells. The spring bloom onset was defined as the first day of year with 5% above the annual median chl *a* concentration over a duration of three or more days (Henson et al., 2009). Due to winter darkness, satellite images were unavailable before 25 January in the south (59.1° N) and 7 March in the north (72.8° N). To avoid a confounding effect between bloom timing and image availability, we disregarded estimates where the bloom onset criteria occurred on the same day as the first available image.

## Statistical analyses

Spatiotemporal changes in observations and estimates were quantified as the slope of simple linear regressions, with the 95% CI given in square brackets. The same linear regressions were also used to quantify the total spatiotemporal ranges.

# RESULTS

Based on the individual field data ($N = 126{,}491$) used as input to the binomial regression model (Equation 1), we note a linear increase in age (0.066 [0.065, 0.067] years per year) and length (0.33 [0.32, 0.34] cm per year) across years (Appendix S1: Figure S1A) and a linear decrease in age (−0.11 [−0.12, −0.10] years per degree latitude) and length (−0.78 [−0.83, −0.73] cm per degree latitude) across latitudes (Appendix S1: Figure S1B). Individuals are most commonly sampled using a gill net, which is consistent across years (Appendix S1: Figure S1C).

The logistic binomial regression model (Equation 1) had a deviance explained of 50.5%–52.5% ($N = 126{,}491$, method = log-likelihood), depending on the initial basis dimension ($k' = 10$, 20, 50 or 150) for the spline-based smooth s($X$, $Y$) (Appendix S1: Table S1). Model predictions of spawning time across year and latitude (see below) did not change significantly for different values of $k'$ (Appendix S1: Table S1), and the remaining results will be based on $k' = 10$ (M_k10, Appendix S1: Table S1). The estimated degrees of freedom (EDF) of the basis dimensions ($k$) for the tensor product smooth *te*(Age, Length) was 5.26. A quantile–quantile plot (Appendix S1: Figure S2A) showed a reasonable 1:1 relationship between model residuals and theoretical quantiles (within ±2 quantiles), with residuals evenly distributed around zero (Appendix S1: Figure S2B). Partial model effects are shown in Appendix S1: Figure S3. Here, we can see that time (Year) and space (Lat, Lon) had the largest effects on spawning time compared to size (Age, Length) and sampling gear (Gear). Also, we found that the observed spatiotemporal trend in age and length (Appendix S1: Figure S1A,B) follow the zero-effect age–length isocline (Appendix S1: Figure S3B), suggesting that model prediction can be done with a constant age–length without bias. Further, we also found that removing predictor variables from the full model (Equation 1) reduced overall model fit (Appendix S1: Table S2).

The model (M_k10) was now used to predict the day of year when there was a 50% probability of the gonad being in spawning stage (Stage = 1), for each of the 253 25 × 25-km grid cells ($X$, $Y$) and 37 years (Year, 1980–2019). Other grid resolutions were also explored but yielded similar predictions (Appendix S1: Table S3). The remaining predictor variables were set to their average value (Age = 8.4 years, Length = 83 cm), except gear type, which was set to the most commonly used gear type (Gear = gill net, Appendix S1: Figure S1C). The statistical model prediction (Figure 2) suggests that spawning has taken place progressively earlier. A simple linear regression suggested an advancement of −7.36 [−8.96, −5.76] days per decade, or a total of 29.4 [23.0, 35.8] days over all years (Table 1). Geographically (59.3–71.9° N), spawning time shifted on average 3.03 [2.62, 3.43] days per degree latitude (Appendix S1: Table S1), or in total

43.9 [38.0, 49.7] days. The binomial logistic relationship between Doy and Stage is shown across years and latitude in Appendix S1: Figure S4.

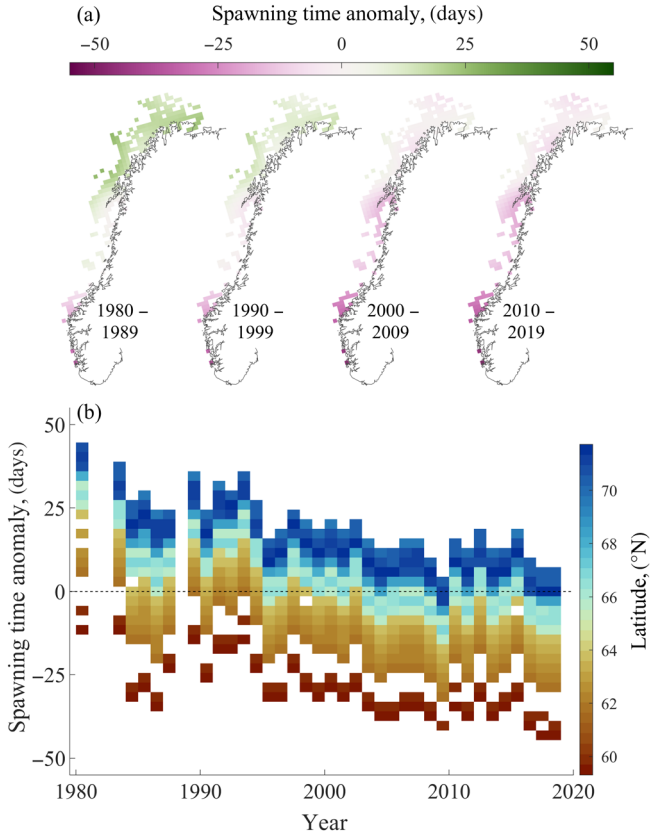


**FIGURE 2** Statistical model prediction of spawning time of Northeast Arctic cod from 1980 to 2019 estimated as day of year when 50% of individuals are in spawning stage (Stage = 1). Panel (a) shows decadal mean spawning time anomaly for each 25 × 25-km grid cell, while panel (b) shows interannual change in spawning time for each latitude (color bar). The following fixed parameters were used in the statistical prediction: Age = 8.4 years, Length = 83 cm, and Gear = gill net.

Starting at the statistical model predictions of spawning time for each year and grid-cell location (Figure 2), we then back-calculated the corresponding vitellogenic temperature ($T_{VIT}$) along each migration route for each year (Figure 3a). This exercise was done following five different assumptions of swimming speed ($v$) as a function of migration distance, $d$ (V1–V5, Appendix S1: Figure S5A). The initial assumption (V1) was a constant speed of 5 km/day ($V_{DST}$), which was the swimming speed that provided a back-calculated $T_{VIT}$ closest to that observed from six DST temperature trajectories recaptured between 69.9 and 71.7° N ($d$ = 450–850 km) in 1997. However, for spawning grounds south of ca 68° N, this low swimming speed yielded migration times between 180 and 460 days, which is unrealistically long. A simple linear relationship (V2), $v(d) = d \times 0.077$, was selected, yielding a maximum speed of 17.7 km/day, with an average $v(d = 450–850\ \text{km}) = 5$ km/day. Three other swimming speed assumptions were also tested (V3–V5, Appendix S1: Figure S5A), and overall results are reported in Appendix S1: Table S4. Of those assumptions yielding realistic migration times (<180 days, V2, V3, and V5, Appendix S1: Figure S5B), the back-calculated $T_{VIT}$ and oocyte development times were not significantly different (Appendix S1: Table S4). An example of $T_{VIT}$ for all grid cells in the years 1996–1997 following swimming speed assumption V2 is shown in Figure 3b.

$T_{VIT}$ was on average 4.3 [4.06, 4.60]°C warmer in the south compared to in the north (Figure 4a and Appendix S1: Table S4), with the temperature-predicted relative spawning time (Figure 4b,c) 19.3 [18.01, 20.63] days earlier in the south compared to in the north (Table 1). Similarly, between 1980 and 2019, $T_{VIT}$ had on average increased by 0.37 [0.25, 0.50]°C per decade, or by 1.49 [0.99, 1.98]°C over the whole period (Appendix S1: Table S4). This warming predicted an advancement in the temperature-dependent relative spawning time by an

**TABLE 1** Summary statistics.

| | Change in spawning time (days) | | Change in spring bloom onset (days) |
|---|---|---|---|
| **Temperature prediction** | **Statistically predicted (Equation 1)** | **Temperature-predicted ($T_{VIT}$, Equation 2)** | **Satellite images** |
| Per decade | | | |
| 1980–2019 | −7.36 [−8.96, −5.96] | −1.67 [−2.26, −1.13] | |
| 1998–2019 | −6.43 [−8.79, −4.08] | −1.88 [−3.22, −0.55] | −8.20 [−9.05, −7.35] |
| Across latitudes | 43.9 [38.0, 49.7] | 19.2 [18.0, 20.6] | 48.9 [46.4, 51.4] |

*Note*: The table summarizes the mean [95% CI] linear change in spawning time derived from a statistical prediction (Equation 1, Figure 2) and a temperature prediction (Equation 2, Figure 3) across years (1980–2019, $N$ = 37 and 1998–2019, $N$ = 22) and latitude (south to north, 59.1° N–72.8° N, $N$ = 48). It also shows the linear change in phytoplankton spring bloom onset across years (1998–2019, $N$ = 22) and latitude (59.3° N–72.8° N, $N$ = 48) derived from satellite images (Figure 6). Statistical estimates of spawning times are based on model (M_k10) predictions on a 25 × 25-km grid (G25). Temperature-predicted relative spawning time is based on the same model and making the V2 swimming speed assumption (Appendix S1: Figure S5 and Table S4).

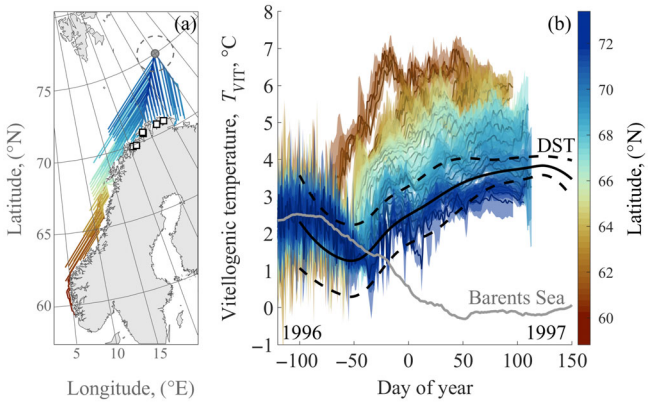


**FIGURE 3** Spawning migration routes and modeled and observed vitellogenic temperatures ($T_{VIT}$). In panel (a), lines denote shortest migration route between central Barents Sea (75° N, 35° E, gray dot) and each 25 × 25-km grid cell ($N = 253$) for which statistical predictions of spawning time were conducted. Color refers to grid-cell latitude. Squares denote recapture locations of six data storage tags (DSTs) in 1997. In panel (b), colored lines and shaded area show mean and 95% CI of back-calculated vitellogenic temperature ($T_{VIT}$) for each latitude (color) from spawning time in 1997 to start of migration in 1996 assuming a V2 swimming speed (Appendix S1: Figure S5). This outline is based on the migration routes in panel (a) and the statistical model predictions (M_k10) of spawning time for each grid cell in 1997 (Figure 2). The solid and dashed black lines denote mean and SD of temperature recorded by the six DSTs. Gray line indicates mean temperature (50–350 m) in central Barents Sea (gray dot in panel a) over whole period.

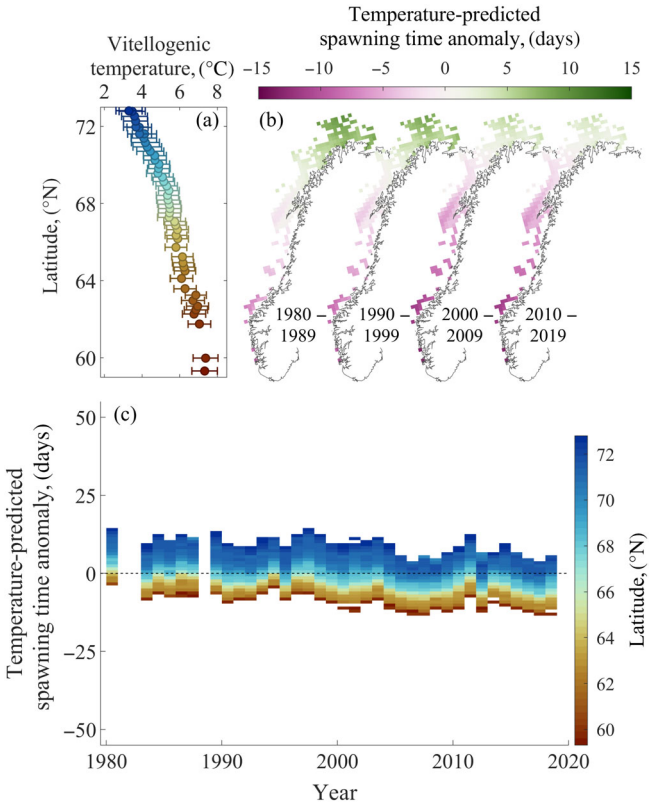


**FIGURE 4** Mechanistic model of vitellogenic temperature and temperature-predicted relative spawning time of Northeast Arctic cod. The vitellogenic temperatures are back-calculated from the statistical model-predicted spawning time in each grid cell for all years (Figure 2) along with the corresponding spawning migration route (Figure 3). (a) Overall mean and 95% CI of $T_{VIT}$ at each grid-cell latitude. (b) Decadal average temperature-predicted spawning time for each grid cell. (c) Interannual change in temperature-predicted spawning time for each grid-cell latitude (color). Temperature-predicted spawning time was calculated based on temperature-dependent oocyte growth rates (Equation 2 using modeled daily $T_{VIT}$ each year and grid cell).

average of −1.69 [−2.26, −1.13] days per decade, or a total of −6.78 [−9.04, −4.52] days from 1980 to 2019 (Figure 4c, Table 1).

From the previously published experiment on the temperature effect on oocyte development (Kjesbu et al., 2010), it is evident that average oocyte growth rates are faster at higher temperatures (Figure 5a, the basis for Equation 1). Although temperature had a significant overall positive effect on oocyte growth rates, the experiment also revealed a large degree of individual variation (Figure 5a). While individuals in warmer water during vitellogenesis (9.3°C) made up the 15% highest ($N = 11$) specific oocyte growth rates and those in colder waters (5°C) made up the 15% lowest ($N = 11$), there was a large degree of overlap in the remaining range (70%, $N = 49$) of intermediate specific oocyte growth rates (Figure 5b). We also note that in colder water, the mean oocyte growth rates for the three "slowest" fish was 2.44 [1.84, 3.03] μm/day ($N = 9$), while for the three "fastest" fish it was 4.92 [4.10, 5.74] μm/day ($N = 8$). This perspective suggests that individual variation in oocyte growth rates can lead to differences in oocyte development times from 250 to 690 μm of around 90 days, or between 181 [146, 240] and 90 [77, 108] days, for individuals with a slow and fast reproductive cycle, respectively.

For the phytoplankton spring bloom, we were able to estimate bloom onset in ca. 90% of the 9361 grid-cell and year combinations. A total of 969 bloom onset estimates (~10%) occurred on the same day as the first available images and were discarded. From the remaining valid estimates we found that across years (1998–2019), the satellite-derived phytoplankton bloom onset occurred on average −8.20 [−9.05, −7.35] days earlier per decade, within a range similar to that of the statistical model prediction for cod spawning time (−6.43 [−8.79, −4.08]) for the same years (Table 1). Likewise, the phytoplankton spring bloom onset was on average 48.9 [46.4, 51.4] days earlier in the south compared to in the north, compared to 43.9 [38.0, 49.7] days from the statistical prediction of

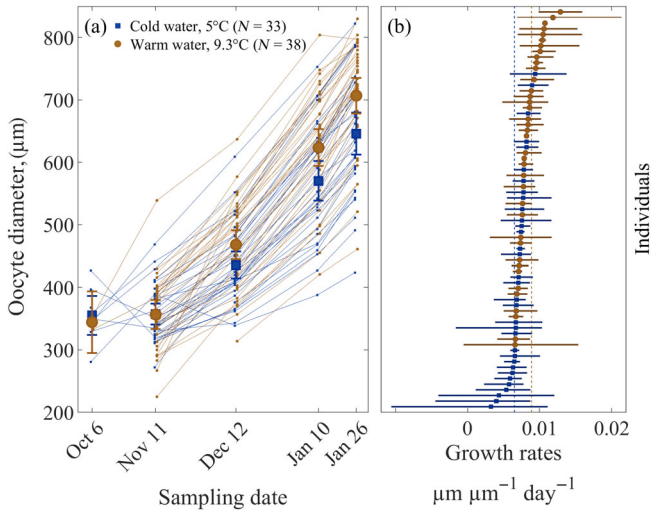


**FIGURE 5** Experimental oocyte growth and oocyte growth rates of coastal cod at different temperature regimes. (a) Temporal development of leading cohort oocyte diameter for 33 and 38 individual cod (thin lines and small symbols), kept at 5°C (blue squares) and 9.3°C (red circles), respectively. The grand mean leading cohort oocyte diameter and 95% CI for each date is denoted by large blue squares (5°C) and large red circles (9.3°C), with error bars. (b) Corresponding individual mean, minimum specific growth rate, and maximum specific growth rate (in micrometers per micrometer per day), in descending order. Dotted vertical lines denote mean specific growth rate at water temperatures of 5°C (blue) and 9.3°C (red). All data originate from Kjesbu et al. (2010).

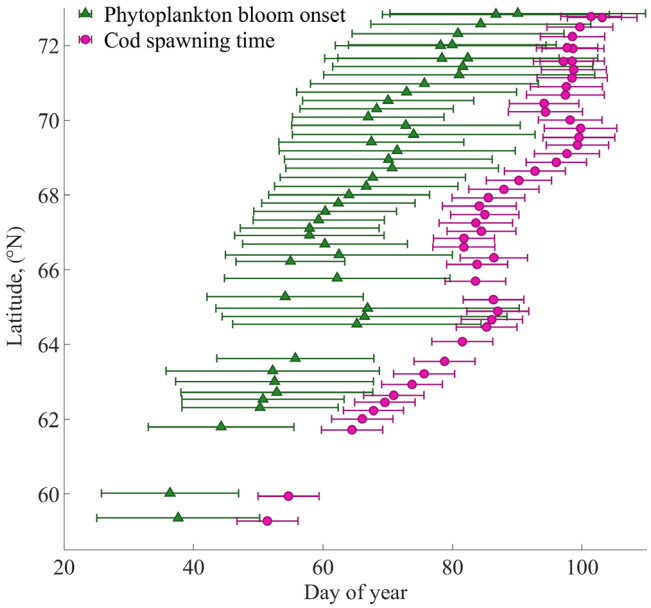


**FIGURE 6** Phytoplankton spring bloom and statistically predicted Northeast Arctic cod spawning time grouped across latitudes. Green triangles and error bars denote mean onset and SD of phytoplankton spring bloom as estimated from satellite images (1998–2019) for each grid-cell latitude. Pink circles and error bars denote corresponding statistical model prediction (Equation 1) of NEA cod spawning time for same latitudes and years. The following fixed parameters were used in the statistical prediction: Age = 8.4 years, Length = 83 cm, and Gear = gill net.

cod spawning time (Figure 6 and Table 1). This latitudinal correspondence in the timing of cod spawning and phytoplankton spring bloom did not appear to be driven by a latitudinal effect on photoperiod (Appendix S1: Figure S6).

## DISCUSSION

Here we have shown that a high degree of trophic synchrony between cod spawning times and the onset of phytoplankton blooms was maintained despite the fact that the latter varied by nearly 50 days across different spawning grounds, as well as advancing by about a week per decade, on average. There was no clear evidence of a gradual decoupling between the phenology of fish spawning and phytoplankton spring bloom as has previously been predicted for other high-latitude areas and fish species (Asch et al., 2019; Poloczanska et al., 2013).

While trophic synchrony between cod spawning and prey production has been indicated when comparing among stocks (Neuheimer et al., 2018; Neuheimer & MacKenzie, 2014), our study details a much finer scale of spatial and temporal matching involving a single migratory stock, implicitly excluding interstock variability. In what follows, we consider possible reasons as to why NEA cod have been able to largely match spawning times with the onset of phytoplankton production during the recent ocean warming, as well as methodological assumptions that may influence our findings.

From the field data we found that the sampled fish were on average 2.6 years older and 13 cm longer in 2019 compared to 1980 and that fish sampled at the most southern spawning grounds were on average 1.4 years older and 11 cm longer compared to those sampled at the northern spawning grounds. The latter is in line with predictions from a state-dependent bioenergetics model, suggesting that natural selection will lead to larger cod spawning farther south (Jørgensen et al., 2008). Interestingly, Pedersen (1984) suggested that an observed reduction in the mean age of the NEA cod spawning stock between 1929 and 1982 was the primary driver of a concurrent 10-day delay in spawning time. Size and age differences in the onset and cessation of spawning gadoids have also been found from experiments (Kjesbu et al., 1996) and the field (Gonzalez-Irusta & Wright, 2016; Rogers & Dougherty, 2019; Wright & Gibb, 2005). Indeed, age

composition rather than temperature was found to explain variation in the time when Newfoundland cod stocks completed spawning (Morgan et al., 2013). However, in this study, spatiotemporal differences in age and length were explicitly accounted for in the model and clearly showed that the observed spatiotemporal change in age/length could not explain the spatiotemporal differences in the statistically predicted spawning time.

The rather dynamic spawning phenology found in this study contrasts with the historical perception that spawning time in NEA cod could be considered fixed in relation to the variable timing of plankton production (Cushing, 1969). The match–mismatch hypothesis (Cushing, 1969, 1990) essentially relies on this assumption when linking offspring survival or recruitment (year–class formation) to changes in the timing of food availability (Endo et al., 2022; Malick et al., 2015; Platt et al., 2003; Schweigert et al., 2013). Any observed differences in peak spawning time of Atlantic cod stocks generally conform to that expected from the temperature-driven vitellogenic oocyte development (Kjesbu et al., 2010; McQueen & Marshall, 2017; Neuheimer & MacKenzie, 2014; Wright, 2013). In this study, the potential link with vitellogenic temperature was explicitly tested. Indeed, warming could partially (23%) explain earlier spawning times with a temperature-predicted change of 1.7 days per decade, compared to the statistically predicted shift of 7.4 days per decade. Likewise, the temperature-predicted effect explained about 44% (19 days) of the statistically predicted 44-day difference in spawning time between north and south. These in-built restrictions in the temperature-predicted effects point to additional factors being involved but are also vulnerable to methodological assumptions.

At the most fundamental level, we assumed that mean oocyte development time could be expressed as a function of temperature (Kjesbu et al., 2010) and, further, that variation in oocyte development time translates to a proportional variation in spawning time. Although the latter is often assumed to be the case (Asch et al., 2019; Kjesbu et al., 2010; Pankhurst & Munday, 2011), one could also consider that individuals can alter the start time of oocyte development and, thus, maintain a fixed spawning time independent of temperature or vary spawning time in constant temperatures. Also, we ignored any potential auxiliary temperature effects on, for example, swimming speed and energetic costs (e.g., Claireaux et al., 1995).

Regarding back-calculation of vitellogenic temperature history, we used tagging data from Godø and Michalsen (2000), together with assumptions on swimming speed, as the starting point of migration, and route selection. Still, certain natural constraints can be used to narrow the possible outcomes. For instance, we know that the NEA cod spawning stock is feeding in the Barents Sea at least until early October (Eriksen et al., 2018), thereby constraining the earliest migration start and effectively eliminating very low swimming speed for southern spawners. Similarly, there are physiological constraints on the upper sustained swimming speed, suggested to be ca. 17 km/day when taking into account that cod swim against a northbound current of ca 8.5 km/day (Jørgensen et al., 2008). When testing various functional relationships between swimming speed and migration distance within these constraints, we found little variation in the back-calculated vitellogenic temperatures. Also, fish are unlikely to swim in a straight line along the shortest possible route. However, considering temperatures were depth-averaged and that the Barents Sea temperature at the starting location is randomly drawn from a temperature distribution representing a 50,000-km$^2$ area, variations in start position and route choice would likely lead to modest changes in the estimates. As such, modeled route and speed should rather be understood as large-scale averages and not representative of individual behavior.

When tracking cod oocyte development in cold and warm water experiments, we found large differences between individuals kept at the same temperature. The outer ranges of these oocyte growth rates translate to an approximately 90-day difference in oocyte development time from 250 to 690 μm. These factual observations speak for the existence of individual variation large enough to explain the discrepancies between the statistical prediction and the temperature prediction of NEA cod spawning time found in this study. This new insight further points to an important weakness when using generalized temperature–response relationships. Although an average effect of temperature on oocyte growth rates can be adequately expressed and mechanistically explained through a $Q_{10}$ temperature coefficient (Kjesbu et al., 2010), the residual individual variation remains unexplained and unaccounted for.

This individual variation observed in the laboratory may provide insight into how NEA cod in the wild can time spawning relative to the phytoplankton bloom timing, somewhat decoupled from temperature constraints. Here, we also found that the bloom occurred on average ca. 3 weeks prior to the time when 50% of the cod were in spawning state. How this translates to the timing of first feeding cod larvae and their food sources, for example, the eggs and nauplii of *C. finmarchicus*, will further depend on a series of additional temperature–development relationships. In Norwegian coastal waters, peak spawning of *C. finmarchicus* occurs around the time of the peak phytoplankton bloom (Broms & Melle, 2007), defined

as the time of maximum depth-integrated chl *a* concentration. While our phytoplankton bloom estimates define the onset and are based on surface concentrations, Opdal et al. (2019) found that surface-average and depth-integrated chl *a* concentrations were correlated and, further, that peak bloom timing occurred 2–3 weeks after onset. This could indicate that the peak of phytoplankton bloom, *Calanus* spawning, and cod spawning occur around the same time. Temperature estimates at the time of both cod and *Calanus* spawning (2–6°C) suggest an additional 2–3 weeks to cod egg hatching and larval first feeding (Geffen et al., 2006; Iversen & Danielssen, 1984), at which point the *Calanus* eggs would already be entering the copepodite stages (Campbell et al., 2001), too large for first feeding cod larvae. This unintuitive offset of 2–3 weeks between the peak of first feeding cod larvae and the peak of their food is puzzling but surprisingly similar to that observed by Ellertsen et al. (1989) at the Lofoten spawning ground. However, Ellertsen et al. (1989) also showed that even if the two peaks did not match in time, there was still considerable overlap between their respective distributions.

While variation in spawning time is responsive to environmental pressures, local adaptation may be expected where there is a strong selective pressure for spawning at a certain time of year. Such local adaptation has been suggested from experiments in Norwegian coastal cod, where fish from different areas that were brought into captivity and held under a common environment regime were found to principally maintain the spawning periodicity of their natal site (Otterå et al., 2012). Local adaptation was also invoked to explain why the migratory component of Icelandic cod stock spawned around the same time as coastal cod, despite experiencing much lower temperatures during vitellogenesis (Grabowski et al., 2011). However, this phenomenon of local adaptations to synchronize spawning time to local bloom timing is apparently widespread, as seen in different populations of Atlantic cod (Neuheimer et al., 2018) and shrimps (Koeller et al., 2009). Thus, the geographical differences in spawning time found in this study could also be explained by genetically distinct subpopulations with subsequent homing behavior. This functional principle could select for evolutionary adaptation to local bloom timing or some other advanced acclimatization mechanism implying, for example, varying $Q_{10}$ values (Schmidt-Nielsen, 2002). Indeed, studies have shown that tagged NEA cod have returned to the same spawning area in two consecutive years (partial homing; Godø, 1984), but the occurrence of true homing, that is, cod returning to their native spawning ground, has, to our knowledge, not yet been investigated.

The experimental data clearly show that, in addition to temperature, specific oocyte growth rate is largely determined by between-individual variation and within individual plasticity. To what degree this variation and plasticity underlies the ability to match spawning time to phytoplankton bloom onset found in the field cannot be inferred by this study, but we note that the observed magnitude in individual variation in the laboratory is sufficient to explain the variation observed in the field. Putting any underlying mechanisms aside, this study has shown a remarkably tight synchrony between fish spawning and bloom timing in both space and time, neither of which can be explained by temperature drivers alone. These findings demonstrate the need for moving beyond the assumption of a purely temperature-driven spawning time and add a new dimension to consider in climate change models predicting future trophic match–mismatch scenarios.

## AUTHOR CONTRIBUTIONS

*Conceptualization*: Anders Frugård Opdal, Peter J. Wright, and Olav Sigurd Kjesbu. *Methodology*: Anders Frugård Opdal, Peter J. Wright, Geir Blom, Christian Lindemann, and Olav Sigurd Kjesbu. *Investigation*: Anders Frugård Opdal, Christian Lindemann, Geir Blom, and Olav Sigurd Kjesbu. *Visualization*: Anders Frugård Opdal. *Writing—original draft*: Anders Frugård Opdal and Peter J. Wright. *Writing—review and editing*: Anders Frugård Opdal, Peter J. Wright, Geir Blom, Hannes Höffle, Christian Lindemann, and Olav Sigurd Kjesbu.

## ACKNOWLEDGMENTS

We thank Tom Williams and Håkon Otterå at the Institute of Marine Research for helping out with the curation and description of the biological data and sampling methods. The work was funded by the following projects: ScaleClim RCN 268336 (Anders Frugård Opdal, Peter J. Wright, Geir Blom, Hannes Höffle, and Olav Sigurd Kjesbu), TerraCoast RCN 287490 (Anders Frugård Opdal, and Christian Lindemann), and SUMMER EU H2020 817806 (Christian Lindemann).

## CONFLICT OF INTEREST STATEMENT

The authors declare no conflicts of interest.

## DATA AVAILABILITY STATEMENT

Data (Opdal et al., 2023) are available in Dryad at https://doi.org/10.5061/dryad.12jm63z2r.

## REFERENCES

Asch, R. G., C. A. Stock, and J. L. Sarmiento. 2019. "Climate Change Impacts on Mismatches between Phytoplankton Blooms and Fish Spawning Phenology." *Global Change Biology* 25: 2544–59.

Atkinson, A., R. A. Harmer, C. E. Widdicombe, A. J. McEvoy, T. J. Smyth, D. G. Cummings, P. J. Somerfield, J. L. Maud, and

K. McConville. 2015. "Questioning the Role of Phenology Shifts and Trophic Mismatching in a Planktonic Food Web." *Progress in Oceanography* 137: 498–512.

Beaugrand, G., K. M. Brander, J. A. Lindley, S. Souissi, and P. C. Reid. 2003. "Plankton Effect on Cod Recruitment in the North Sea." *Nature* 426: 661–64.

Bergstad, O. A., T. Jørgensen, and O. Dragesund. 1987. "Life-History and Ecology of the Gadoid Resources of the Barents Sea." *Fisheries Research* 5: 119–161.

Both, C., S. Bouwhuis, C. M. Lessells, and M. E. Visser. 2006. "Climate Change and Population Declines in a Long-Distance Migratory Bird." *Nature* 441: 81–83.

Both, C., M. van Asch, R. G. Bijlsma, A. B. van den Burg, and M. E. Visser. 2009. "Climate Change and Unequal Phenological Changes across Four Trophic Levels: Constraints or Adaptations?" *Journal of Animal Ecology* 78: 73–83.

Broms, C., and W. Melle. 2007. "Seasonal Development of *Calanus finmarchicus* in Relation to Phytoplankton Bloom Dynamics in the Norwegian Sea." *Deep-Sea Research Part II-Topical Studies in Oceanography* 54: 2760–75.

Campbell, R. G., M. M. Wagner, G. J. Teegarden, C. A. Boudreau, and E. G. Durbin. 2001. "Growth and Development Rates of the Copepod *Calanus finmarchicus* Reared in the Laboratory." *Marine Ecology Progress Series* 221: 161–183.

Claireaux, G., D. M. Webber, S. R. Kerr, and R. G. Boutilier. 1995. "Physiology and Behavior of Free-Swimming Atlantic Cod (*Gadus morhua*) Facing Fluctuating Temperature Conditions." *Journal of Experimental Biology* 198: 49–60.

Cushing, D. H. 1969. "Regularity of Spawning Season of some Fishes." *Journal du Conseil* 33: 81–92.

Cushing, D. H. 1990. "Plankton Production and Year-Class Strength in Fish Populations—An Update of the Match Mismatch Hypothesis." *Advances in Marine Biology* 26: 249–293.

Denechaud, C., A. J. Geffen, S. Smoliński, and J. A. Godiksen. 2021. "Otolith "Spawning Zones" across Multiple Atlantic Cod Populations: Do they Accurately Record Maturity and Spawning?" *PLoS One* 16: e0257218.

Doney, S. C. 2006. "Oceanography—Plankton in a Warmer World." *Nature* 444: 695–96.

Durant, J. M., D. O. Hjermann, G. Ottersen, and N. C. Stenseth. 2007. "Climate and the Match or Mismatch between Predator Requirements and Resource Availability." *Climate Research* 33: 271–283.

Edwards, M., and A. J. Richardson. 2004. "Impact of Climate Change on Marine Pelagic Phenology and Trophic Mismatch." *Nature* 430: 881–84.

Ellertsen, B., P. Fossum, P. Solemdal, and S. Sundby. 1989. "Relations between Temperature and Survival of Eggs and First Feeding Larvae of the North-East Arctic Cod (*Gadus morhua L.*)." *Rapports et Procès-verbaux des Réunions, Conseil International pour l'Exploration de la Mer* 19: 209–219.

Endo, C. A. K., L. C. Stige, M. D. Skogen, L. Ciannelli, and F. V. Vikebø. 2022. "Two Decades of Match-Mismatch in Northeast Arctic Cod—Feeding Conditions and Survival." *Frontiers in Marine Science* 9: 767290.

Eriksen, E., H. Gjøsæter, D. Prozorkevich, E. Shamray, A. Dolgov, M. Skern-Mauritzen, J. E. Stiansen, Y. Kovalev, and K. Sunnana. 2018. "From Single Species Surveys towards Monitoring of the Barents Sea Ecosystem." *Progress in Oceanography* 166: 4–14.

Fangel, K., O. Aas, J. H. Vølstad, K. M. Bærum, S. Christensen-Dalsgaard, K. Nedreaas, M. Øvervik, L. C. Wold, and T. Anker-Nilssen. 2015. "Assessing Incidental Bycatch of Seabirds in Norwegian Coastal Commercial Fisheries: Empirical and Methodological Lessons." *Global Ecology and Conservation* 4: 127–136.

Garnesson, P., and M. Bretagnon. 2022. "QUID for OC TAC Products OCEANCOLOUR OBSERVATIONS GlobColour." Copernicus Marine Service.

Geffen, A. J., C. J. Fox, and R. D. M. Nash. 2006. "Temperature-Dependent Development Rates of Cod *Gadus morhua* Eggs." *Journal of Fish Biology* 69: 1060–80.

Godø, O. R. 1984. "Migration, Mingling and Homing of North-East Arctic Cod from Two Separated Spawning Grounds." In *Reproduction and Recruitment of Arctic Cod*, edited by O. R. Godø and S. Tilseth, 289–302. Bergen, Norway: Institute of Marine Research.

Godø, O. R., and K. Michalsen. 2000. "Migratory Behaviour of North-East Arctic Cod, Studied by Use of Data Storage Tags." *Fisheries Research* 48: 127–140.

Gonzalez-Irusta, J. M., and P. J. Wright. 2016. "Spawning Grounds of Atlantic Cod (*Gadus morhua*) in the North Sea." *ICES Journal of Marine Science* 73: 304–315.

Grabowski, T. B., V. Thorsteinsson, B. J. McAdam, and G. Marteinsdottir. 2011. "Evidence of Segregated Spawning in a Single Marine Fish Stock: Sympatric Divergence of Ecotypes in Icelandic Cod?" *PLoS One* 6: e17528.

Hart, P. E., N. J. Nilsson, and B. Raphael. 1968. "A Formal Basis for Heuristic Determination of Minimum Cost Paths." *IEEE Transactions on Systems Science and Cybernetics* 4: 100–107.

Henson, S. A., J. P. Dunne, and J. L. Sarmiento. 2009. "Decadal Variability in North Atlantic Phytoplankton Blooms." *Journal of Geophysical Research-Oceans* 114: C04013.

Hjort, J. 1914. "Fluctuations in the Great Fisheries of Northern Europe Viewed in the Light of Biological Research." *Rapports et Procès-verbaux des Réunions, Conseil International pour l'Exploration de la Mer* 20: 1–228.

Hughes, L. 2000. "Biological Consequences of Global Warming: Is the Signal Already Apparent?" *Trends in Ecology & Evolution* 15: 56–61.

Iversen, S. A., and D. S. Danielssen. 1984. "Development and Mortality of Cod (*Gadus morhua L.*) Eggs and Larvae in Different Temperatures." In *The Propagation of Cod Gadus morhua L. Flødevigen Rapportserie*, edited by E. Dahl, D. S. Danielssen, E. Moksness, and P. Solemdal, 49–65. Bergen: Institute of Marine Research.

Jørgensen, C., E. S. Dunlop, A. F. Opdal, and Ø. Fiksen. 2008. "The Evolution of Spawning Migrations: State Dependence and Fishing-Induced Changes." *Ecology* 89: 3436–48.

Kjesbu, O. S., M. Alix, A. B. Sandø, E. Strand, P. J. Wright, D. G. Johns, A. Thorsen, et al. 2023. "Latitudinally Distinct Stocks of Atlantic Cod Face Fundamentally Different Biophysical Challenges under on-Going Climate Change." *Fish and Fisheries* 2: 297–320.

Kjesbu, O. S., C. T. Marshall, D. Righton, M. Krüger-Johnsen, A. Thorsen, K. Michalsen, M. Fonn, and P. R. Witthames. 2010. "Thermal Dynamics of Ovarian Maturation in Atlantic Cod

(*Gadus morhua*)." *Canadian Journal of Fisheries and Aquatic Sciences* 67: 605–625.

Kjesbu, O. S., P. Solemdal, P. Bratland, and M. Fonn. 1996. "Variation in Annual Egg Production in Individual Captive Atlantic Cod (*Gadus morhua*)." *Canadian Journal of Fisheries and Aquatic Sciences* 53: 610–620.

Koeller, P., C. Fuentes-Yaco, T. Platt, S. Sathyendranath, A. Richards, P. Ouellet, D. Orr, et al. 2009. "Basin-Scale Coherence in Phenology of Shrimps and Phytoplankton in the North Atlantic Ocean." *Science* 324: 791–93.

Kristiansen, T., K. F. Drinkwater, R. G. Lough, and S. Sundby. 2011. "Recruitment Variability in North Atlantic Cod and Match-Mismatch Dynamics." *PLoS One* 6: e17456. https://doi.org/10.1371/journal.pone.0017456.

Lien, V. S., Y. Gusdal, J. Albretsen, A. Melsom, and F. B. Vikebø. 2013. "Evaluation of a Nordic Seas 4 Km Numerical Ocean Model Hindcast Archive (SVIM), 1960-2011." *Fisken og havet* 7: 1–82.

Lien, V. S., Y. Gusdal, and F. B. Vikebø. 2014. "Along-Shelf Hydrographic Anomalies in the Nordic Seas (1960–2011): Locally Generated or Advective Signals?" *Ocean Dynamics* 64: 1047–59.

Lindemann, C., and M. A. St. John. 2014. "A Seasonal Diary of Phytoplankton in the North Atlantic." *Frontiers in Marine Science* 1: 37. https://doi.org/10.3389/fmars.2014.00037.

Malick, M. J., S. P. Cox, F. J. Mueter, R. M. Peterman, and M. Bradford. 2015. "Linking Phytoplankton Phenology to Salmon Productivity along a North–South Gradient in the Northeast Pacific Ocean." *Canadian Journal of Fisheries and Aquatic Sciences* 72: 697–708.

McQueen, K., and C. T. Marshall. 2017. "Shifts in Spawning Phenology of Cod Linked to Rising Sea Temperatures." *ICES Journal of Marine Science* 74: 1561–73.

Melle, W., J. A. Runge, E. Head, S. Plourde, C. Castellani, P. Licandro, J. Pierson, et al. 2014. "The North Atlantic Ocean as Habitat for *Calanus finmarchicus*: Environmental Factors and Life History Traits." *Progress in Oceanography* 129: 244–284.

Moan, A., M. Skern-Mauritzen, J. H. Vølstad, and A. Bjørge. 2020. "Assessing the Impact of Fisheries-Related Mortality of Harbour Porpoise (*Phocoena phocoena*) Caused by Incidental Bycatch in the Dynamic Norwegian Gillnet Fisheries." *ICES Journal of Marine Science* 77: 3039–49.

Morgan, M. J., P. J. Wright, and R. M. Rideout. 2013. "Effect of Age and Temperature on Spawning Time in Two Gadoid Species." *Fisheries Research* 138: 42–51.

Neuheimer, A. B., and B. R. MacKenzie. 2014. "Explaining Life History Variation in a Changing Climate across a species' Range." *Ecology* 95: 3364–75.

Neuheimer, A. B., B. R. MacKenzie, and M. R. Payne. 2018. "Temperature-Dependent Adaptation Allows Fish to Meet their Food across their Species' Range." *Science Advances* 4: eaar4349.

Opdal, A. F., and C. Jørgensen. 2015. "Long Term Change in a Behavioural Trait: Truncated Spawning Distribution and Demography in Northeast Arctic Cod." *Global Change Biology* 21: 1521–30.

Opdal, A. F., C. Lindemann, and D. L. Aksnes. 2019. "Centennial Decline in North Sea Water Clarity Causes Strong Delay in Phytoplankton Bloom Timing." *Global Change Biology* 25: 3946–53.

Opdal, A. F., and F. B. Vikebø. 2016. "Long-Term Stability in Modelled Zooplankton Influx Could Uphold Major Fish Spawning Grounds on the Norwegian Continental Shelf." *Canadian Journal of Fisheries and Aquatic Sciences* 73: 189–196.

Opdal, A. F., P. J. Wright, G. Blom, H. Höffle, C. Lindemann, and O. S. Kjesbu. 2023. "Dataset for: Spawning Fish Maintains Trophic Synchrony across Time and Space beyond Thermal Drivers." Dryad, Dataset. https://doi.org/10.5061/dryad.12jm63z2r.

Otterå, H., A. L. Agnalt, A. Thorsen, O. S. Kjesbu, G. Dahle, and K. Jørstad. 2012. "Is Spawning Time of Marine Fish Imprinted in the Genes? A Two-Generation Experiment on Local Atlantic Cod (*Gadus morhua* L.) Populations from Different Geographical Regions." *ICES Journal of Marine Science* 69: 1722–28.

Pankhurst, N. W., and P. L. Munday. 2011. "Effects of Climate Change on Fish Reproduction and Early Life History Stages." *Marine and Freshwater Research* 62: 1015–26.

Parmesan, C. 2007. "Influences of Species, Latitudes and Methodologies on Estimates of Phenological Response to Global Warming." *Global Change Biology* 13: 1860–72.

Pedersen, T. 1984. "Variation in Peak Spawning of Arcto-Norwegian Cod (*Gadus morhua L.*) during the Time Period 1929-1982 Based on Indices Estimated from Fishery Statistics." In *The Propagation of Cod, Gadus morhua L. Flødevigen Rapportserie*, edited by E. Dahl, D. S. Danielssen, E. Moksness, and P. Solemdal, 301–316. Bergen: Institute of Marine Research.

Platt, T., C. Fuentes-Yaco, and K. T. Frank. 2003. "Spring Algal Bloom and Larval Fish Survival." *Nature* 423: 398–99.

Poloczanska, E. S., C. J. Brown, W. J. Sydeman, W. Kiessling, D. S. Schoeman, P. J. Moore, K. Brander, et al. 2013. "Global Imprint of Climate Change on Marine Life." *Nature Climate Change* 3: 919–925.

Rogers, L. A., and A. B. Dougherty. 2019. "Effects of Climate and Demography on Reproductive Phenology of a Harvested Marine Fish Population." *Global Change Biology* 25: 708–720.

Rollefsen, G. 1933. "The Otoliths of the Cod." Preliminary Report. Fiskeridirektoratets Skrifter. Serie Havundersøkelser (Report of the Norwegian Fisheries and Marine investigations). 4:3–14.

Samplonius, J. M., A. Atkinson, C. Hassall, K. Keogan, S. J. Thackeray, J. J. Assmann, M. D. Burgess, et al. 2021. "Strengthening the Evidence Base for Temperature-Mediated Phenological Asynchrony and its Impacts." *Nature Ecology & Evolution* 5: 155–164.

Schmidt-Nielsen, K. 2002. *Animal Physiology: Adaptation and Environment*, 5th ed. Cambridge: Cambridge University Press.

Schweigert, J. F., M. Thompson, C. Fort, D. E. Hay, T. W. Therriault, and L. N. Brown. 2013. "Factors Linking Pacific Herring (*Clupea pallasi*) Productivity and the Spring Plankton Bloom in the Strait of Georgia, British Columbia, Canada." *Progress in Oceanography* 115: 103–110.

Sundby, S., K. F. Drinkwater, and O. S. Kjesbu. 2016. "The North Atlantic Spring-Bloom System—Where the Changing Climate Meets the Winter Dark." *Frontiers in Marine Science* 3: 28.

Sverdrup, H. U. 1953. "On Conditions for the Vernal Blooming of Phytoplankton." *Journal de Conseil* 18: 287–295.

Thackeray, S. J., P. A. Henrys, D. Hemming, J. R. Bell, M. S. Botham, S. Burthe, P. Helaouet, et al. 2016. "Phenological Sensitivity to Climate across Taxa and Trophic Levels." *Nature* 535: 241–45.

van der Meeren, T., and V. P. Ivannikov. 2006. "Seasonal Shift in Spawning of Atlantic Cod (*Gadus morhua* L.) by Photoperiod Manipulation: Egg Quality in Relation to Temperature and Intensive Larval Rearing." *Aquaculture Research* 37: 898–913.

Winder, M., and D. E. Schindler. 2004. "Climate Change Uncouples Trophic Interactions in an Aquatic Ecosystem." *Ecology* 85: 2100–2106.

Wood, S. N., N. Pya, and B. Säfken. 2016. "Smoothing Parameter and Model Selection for General Smooth Models (with Discussion)." *Journal of the American Statistical Association* 111: 1548–75.

Wright, P. J. 2013. "Methodological Challenges to Examining the Causes of Variation in Stock Reproductive Potential." *Fisheries Research* 138: 14–22.

Wright, P. J., and F. M. Gibb. 2005. "Selection for Birth Date in North Sea Haddock and its Relation to Maternal Age." *Journal of Animal Ecology* 74: 303–312.

## SUPPORTING INFORMATION

Additional supporting information can be found online in the Supporting Information section at the end of this article.

**How to cite this article:** Opdal, Anders Frugård, Peter J. Wright, Geir Blom, Hannes Höffle, Christian Lindemann, and Olav Sigurd Kjesbu. 2024. "Spawning Fish Maintains Trophic Synchrony across Time and Space beyond Thermal Drivers." *Ecology* 105(6): e4304. https://doi.org/10.1002/ecy.4304